

SUPPLEMENTAL INFORMATION

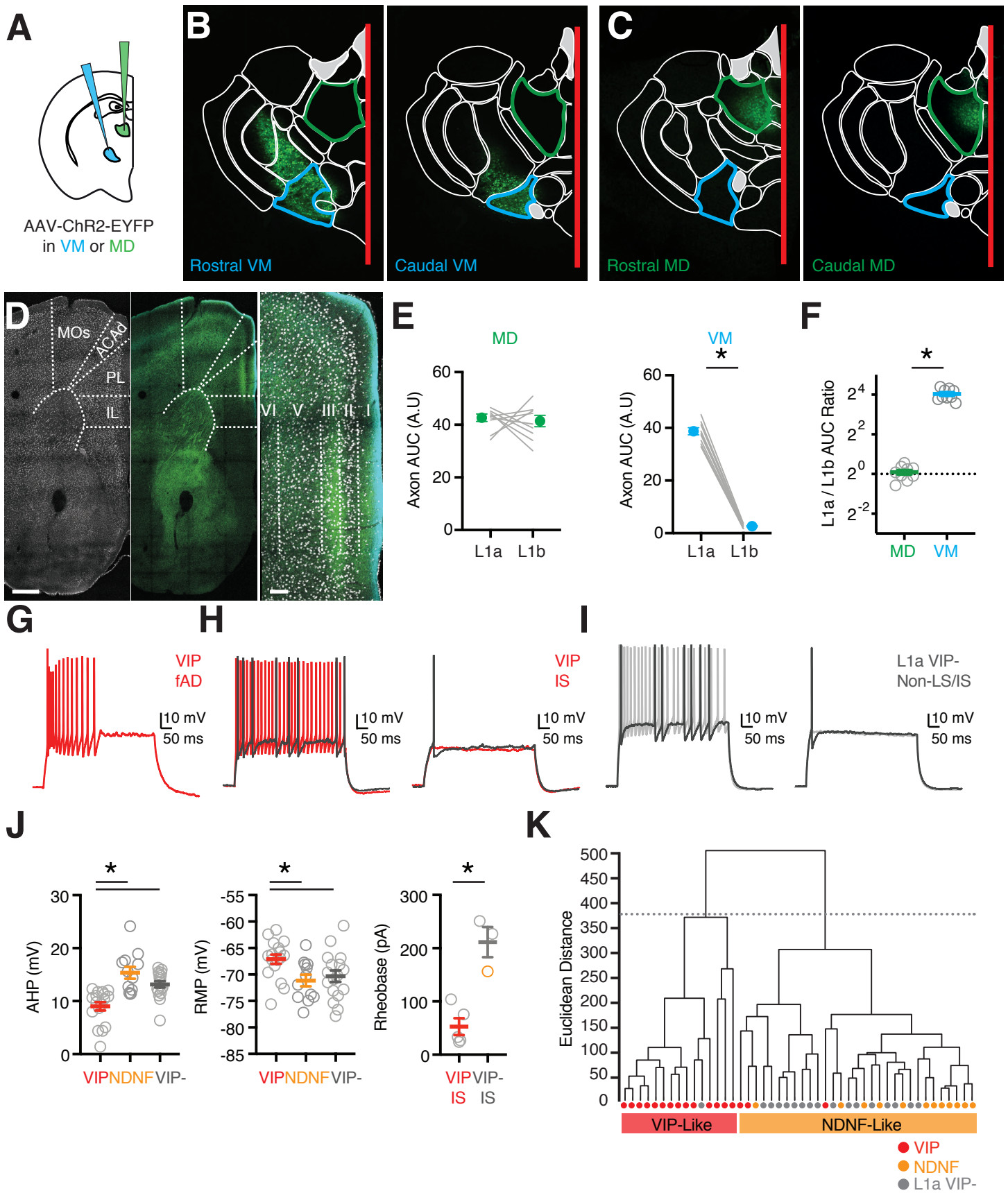
Figure S1. Thalamus anatomy and interneuron firing properties, relates to figure 1

- (A) Injection schematic for AAV-ChR2-EYFP injection into MD or VM.
- (B) Representative VM injection site showing the distribution of ChR2+ / EYFP+ neurons at rostral and caudal subdivisions of VM (Allen Brain atlas slice 66 and 69 respectively). VM is highlighted in blue and MD in green.
- (C) Representative MD injection site showing the distribution of ChR2+ / EYFP+ neurons at rostral and caudal subdivisions of MD (Allen Brain atlas slice 65 and 69 respectively). VM is highlighted in blue and MD in green.
- (D) Location of thalamic axon across subdivisions of frontal cortex and layers of prelimbic PFC. Left: DAPI stain showing the subdivision of PFC into infralimbic (IL), prelimbic (PL) dorsal cingulate cortex (ACAd) and adjacent secondary motor cortex (MOs) Scale bar: 500 μ m. Middle: Distribution of MD (green) and VM (blue) axon across different regions of the frontal cortex. Right: Close up showing the distribution of MD and VM axon across layers of PFC, in addition to L1 there is a dense band of MD axon in L3. Scale bar = 100 μ m.
- (E) Left: Relative axon density calculated as the area under the curve (AUC) of the axon fluorescent intensity profile for MD axon in L1a and L1b. Right: Similar but for VM.
- (F) Ratio of axon AUC in L1a / L1b for MD and VM. Note the logarithmic y axis.
- (G) Example of L1 VIP+ fast adapting (fAD) interneuron firing properties.
- (H) Examples of L1 VIP+ irregular spiking (IS) interneuron firing properties. Left: Dark trace shows peri-threshold spike and red trace shows response to larger current injection. Right: Dark trace shows suprathreshold spike and red trace just sub-threshold response.
- (I) Similar to (B) for L1a VIP- IS neuron.

(J) Summary of L1 interneuron intrinsic properties. From left to right: amplitude of after hyperpolarization (AHP), resting membrane potential (RMP), and rheobase current for VIP+ IS cells and VIP- (NDNF+) IS cells. Data points are individual cells.

(K) Hierarchical clustering of interneuron intrinsic properties indicating that they segregate into two main clusters (dashed line), one containing primarily VIP+ interneurons and the other L1a NDNF+ or VIP- interneurons.

Values are mean \pm SEM (E, J) or geometric mean \pm 95% CI (F). * = $p < 0.05$.



Anastasiades et al., Figure S1

Figure S2. Whole-brain rabies inputs to VIP+ and NDNF+ interneurons, relates to figure 2

(A) Top: Summary of the percentage of starter cells in different subregions of the PFC: anterior cingulate cortex (ACC), prelimbic cortex (PL) and infralimbic cortex (IL). Bottom: Summary of the number of presynaptically labeled GFP+ cells vs. the number of starter cells in NDNF-Cre and VIP-Cre mice.

(B) Top: Normalized rostro-caudal distributions of presynaptic GFP+ labeled cells from NDNF-Cre mice broken down into the main cortical and subcortical brain regions. Bottom: Similar but for VIP-Cre mice. Ctx = cortex, S & P = striatum and pallidum, Hipp = hippocampus, Amyg = amygdala, Cla = claustrum, Olf = olfactory regions, Hypo = hypothalamus, M & H = midbrain and hindbrain, Thal = thalamus.

(C) Representative images showing labeling of presynaptic GFP+ neurons in key brain regions. Scale bar: 100 μ m.

(D) Summary of the percentage of presynaptic cells localized to different subregions of the striatum and pallidum in NDNF-Cre and VIP-Cre mice. NDB / MA = diagonal band nucleus / magnocellular nucleus, GP = globus pallidus, LS = lateral septum, SI = substantia innominate, MS = medial septum, DMSTR = dorsomedial striatum, SH = septohippocampal nucleus, NAC = nucleus accumbens.

Values are mean \pm SEM (D). * = $p < 0.05$.

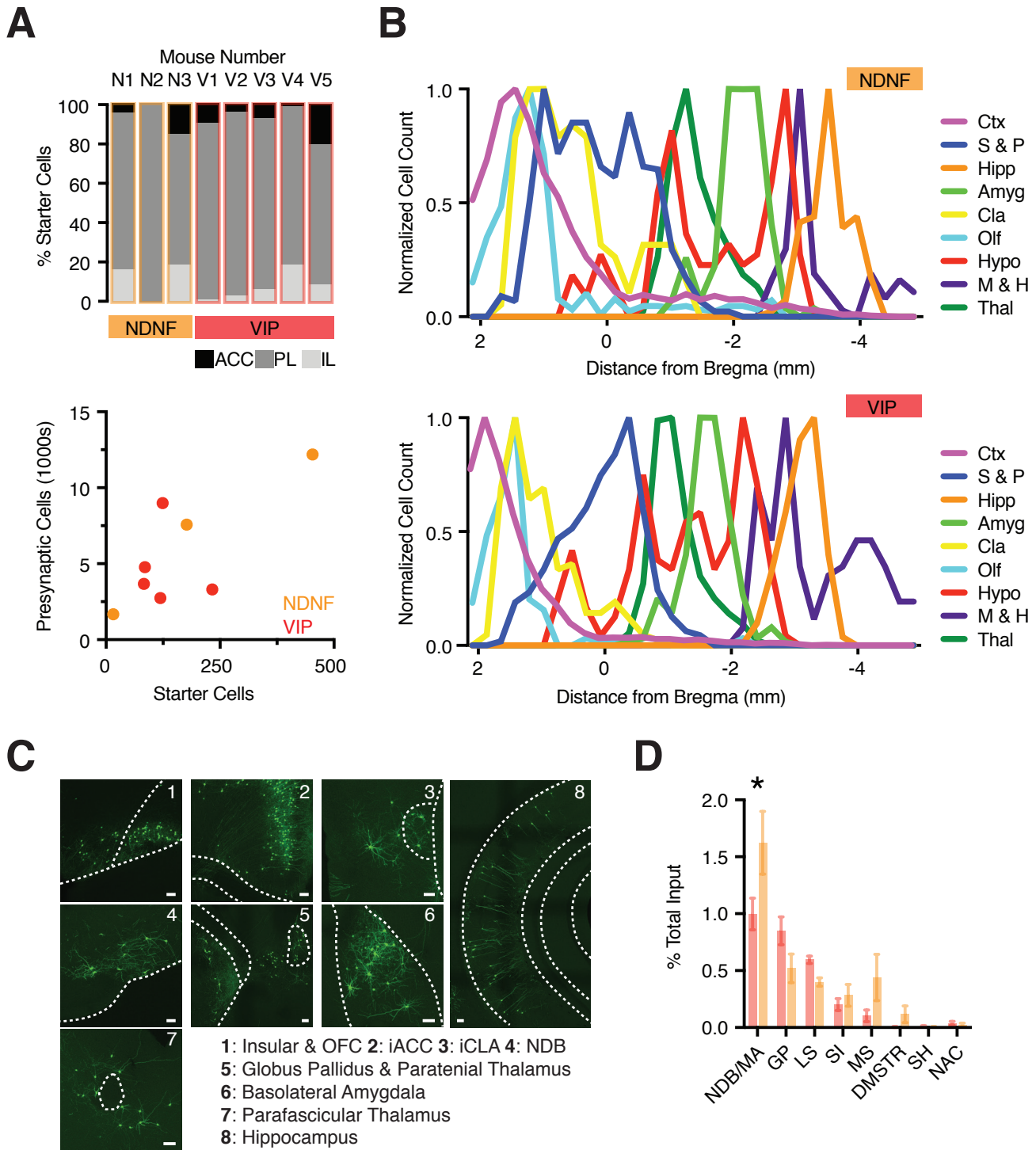


Figure S3. Cortical and thalamic rabies inputs to VIP+ and NDNF+ interneurons, relates to figure 2

(A) Representative images showing labeling of presynaptic GFP+ neurons in key cortical regions.

Scale bar: 100 μ m. SSp = primary somatosensory cortex, Ptlp = posterior parietal association area, TEA = temporal association area, Aud = auditory cortex, ACC = anterior cingulate, MOs = secondary motor cortex, MOp = primary motor cortex, RSPv = ventral retrosplenial cortex.

(B) Left: Summary of percentage of cortical input derived from different cortical regions. Right:

Summary of the percentage of ipsilateral and contralateral cortical input from individual subdivisions of the PFC. PL = prelimbic cortex, IL = infralimbic cortex, ORB = orbital cortex.

(C) Summary of percentage of thalamic input derived from different thalamic clusters (see Philips et al., 2019 for nomenclature).

Values are mean \pm SEM (B,C). * = $p < 0.05$

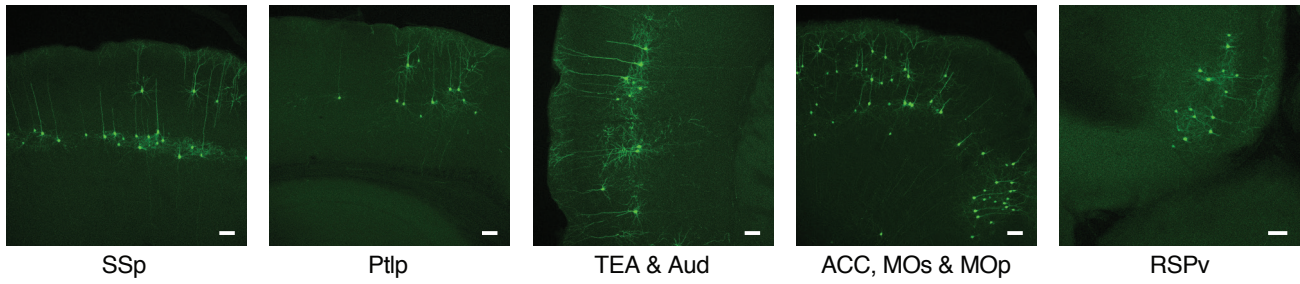
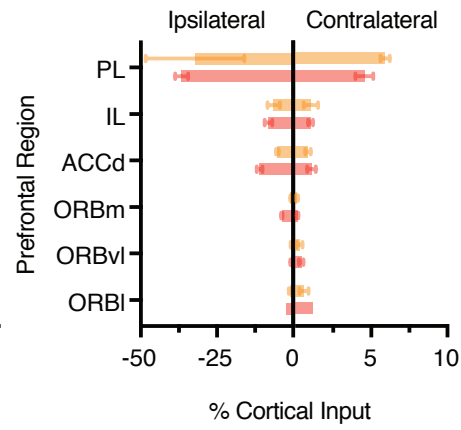
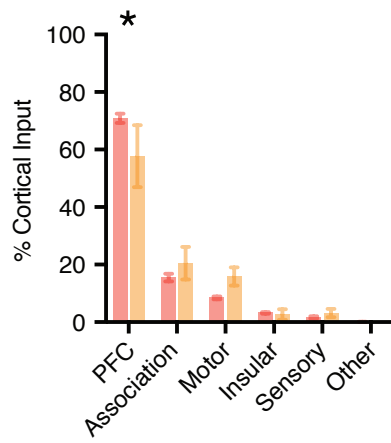
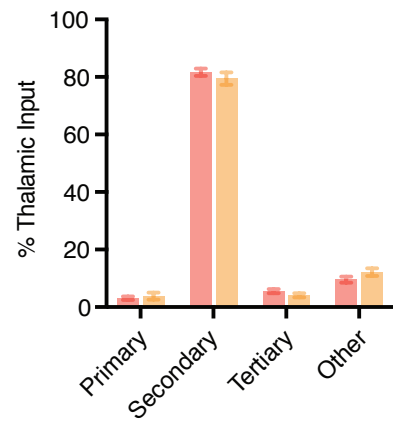
A**B****C**

Figure S4. Properties of VIP+ and NDNF+ synapses in the PFC, relates to figure 4

- (A)** Left: Schematic of labeled cells. Right: Example firing properties of (left to right): L2/3 PYR neuron, PV+ interneuron labeled in G42 mouse, and SOM+ interneuron labeled in GIN mouse.
- (B)** Left: Average IPSCs for NDNF+ → PYR (black), NDNF+ → PV+ (green) and VIP+ → SOM+ (purple) connections. NDNF+ traces have been peak scaled to the VIP+ → SOM+ trace. Right: Expanded view of traces shown at left. Note the onset and time to peak of NDNF+ outputs.
- (C)** Left: Summary of IPSC charge for VIP+ connections. Right: Summary of IPSC charge for NDNF+ connections.
- (D)** Current-clamp recordings showing the average fast and slow component of NDNF-mediated IPSPs at PYRs (left) and PV+ interneurons (right). The slow component was calculated by subtracting the fast IPSP recorded in the presence of CGP from the control IPSP.
- (E)** Left: Summary showing percentage reduction of the fast IPSP peak by bath application of GZ. Right: Similar for reduction of the slow IPSP peak by bath application of CGP. The fast IPSP is reduced by GZ and the slow IPSP by CGP.

Values are mean ± SEM (C,E). * = $p < 0.05$

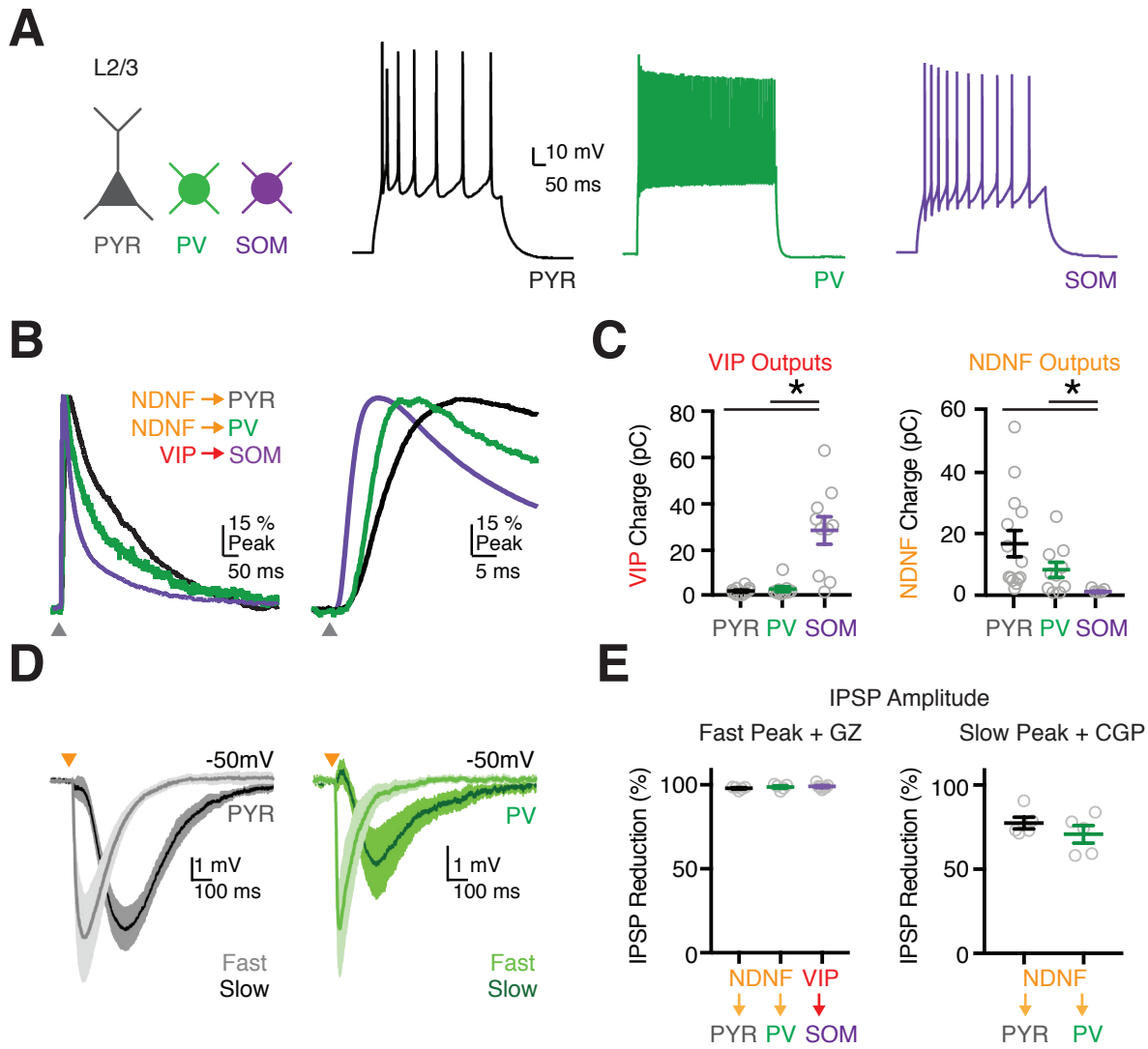


Figure S5. Interneuron outputs to pyramidal cells and L2/3 SOM+ interneurons, relates to figure 5

(A) Summary of NDNF+ IPSC amplitude recorded from triplets of PYR, IT and PT cells.

(B) Summary of NDNF+ IPSC decay constant recorded from triplets of PYR, IT and PT cells.

(C) Top left: Recording schematic, showing grid of light spots. Top right: Light-evoked action potentials (APs) in cell-attached mode from an VIP+ st-ChroME+ cell. Blue bar shows light stimulation. Bottom: Summary of light-evoked APs per pixel as a function of distance from the soma for all VIP+ st-ChroME+ cells recorded in cell-attached mode.

(D) Left: Recording schematic, showing grid of light spots. Middle: Normalized maps of VIP-evoked IPSCs at L2/3 SOM+ cells, indicating location of presynaptic VIP+ cells. Circles show soma depth of recorded cells in L2/3. Individual pixels are 75 x 75 μm . Right: Representative examples of VIP-evoked IPSCs at different layers. Light traces are individual traces and dark traces are averages. Blue bar shows light stimulation.

Values are mean \pm SEM (A, B, C). * = $p < 0.05$.

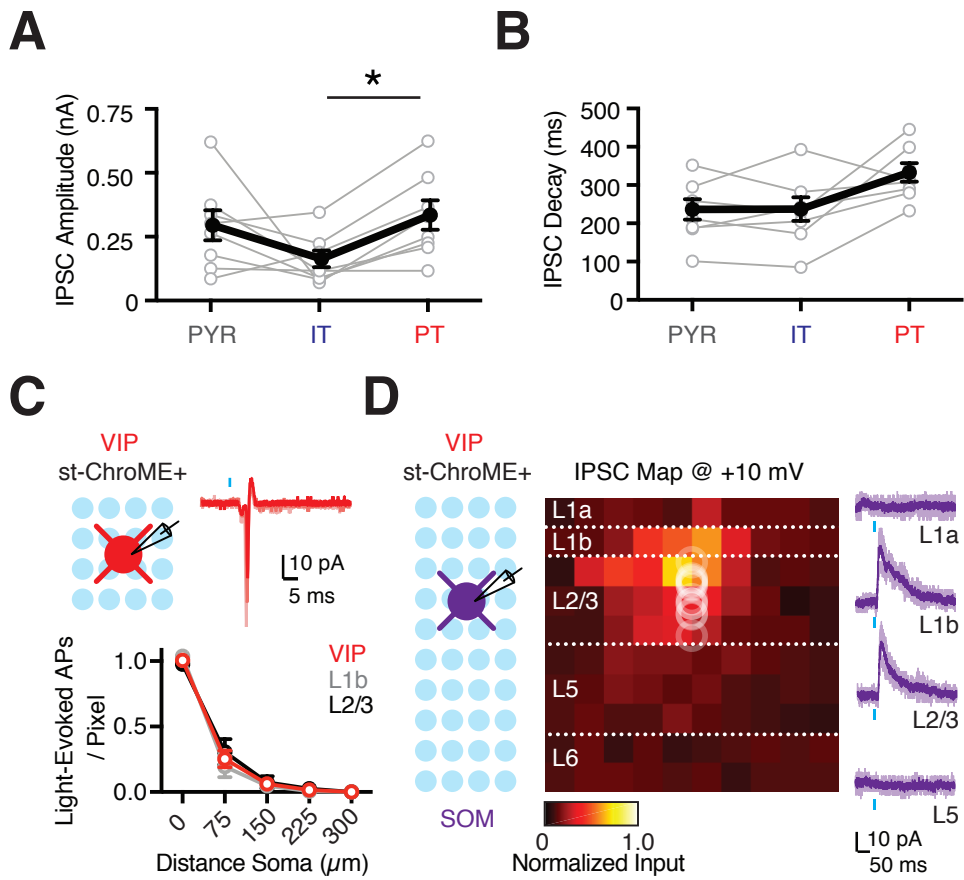


Figure S6. NDNF+ interneurons target apical dendrites of IT cells to regulate Ca²⁺ signals, relates to figure 6

- (A) Summary of dendrite density as a function of distance from the pial surface for IT and PT cells.
- (B) Left: Recording schematic, showing grid of light spots. Middle: Normalized NDNF+ sCRACM connectivity map for light-evoked IPSCs onto IT neurons recorded in the presence of TTX and 4-AP at +10 mV. Individual triangles represent soma depth of recorded IT cells. Right: Representative examples of evoked responses, showing three traces recorded from an individual cell for an individual light spot and the average of those traces (dark trace). Individual pixels are 75 x 75 μm .
- (C) Current-clamp recordings from IT cells in response to 3 bAPs at 100 Hz suprathreshold electrical stimulation at the soma paired with optogenetic stimulation of NDNF+ interneurons over apical or basal dendrites.
- (D) 2-photon imaging of Ca²⁺ signals in the apical and basal dendrites in response to 3 bAPs at 100 Hz, as shown in (C). Traces are shown for trials with and without NDNF+ stimulation.
- (E) Current-clamp recordings from PT cells (top) or IT cells (bottom) in response to 3 bAPs at 100 Hz suprathreshold electrical stimulation at the soma paired with optogenetic stimulation of NDNF+ interneurons over the apical oblique dendrites.
- (F) 2-photon imaging of Ca²⁺ signals in the apical oblique dendrites in response to 3 bAPs at 100 Hz, as shown in (E). Average traces are shown for trials with and without NDNF+ stimulation for PT (left) and IT (right) cells.
- (G) Impact of NDNF+ stimulation on dendritic bAP-evoked Ca²⁺ signals as a function of distance from the soma in IT and PT cells. Summary showing the fraction of the Ca²⁺ signal suppressed by NDNF+ stimulation at different dendritic locations. Data is pooled across apical, basal and oblique dendrites. Ca²⁺ signals are strongly suppressed in distal dendrites but not those close to the soma.

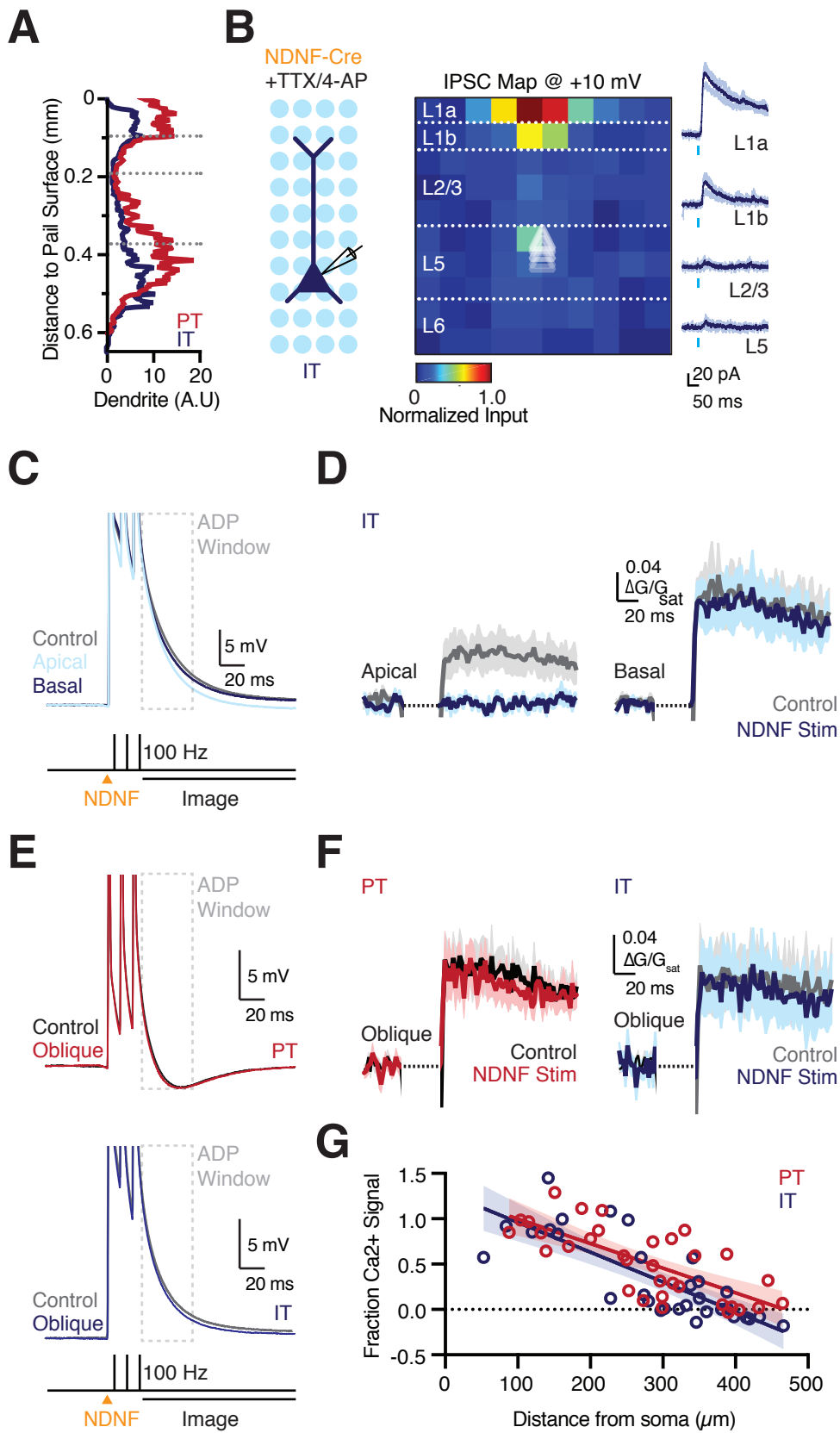


Figure S7. VM selectively targets apical dendrites of PT cells, relates to figure 7

- (A)** Left: Recording schematic, showing grid of light spots. Middle: Normalized VM sCRACM connectivity map for light-evoked EPSCs onto IT cells recorded in the presence of TTX and 4-AP at -70 mV. Individual triangles represent soma depth of recorded IT cells. Right: Examples of light-evoked EPSCs from individual layers. Representative examples of evoked responses, showing three traces recorded from an individual cell for an individual light spot and the average of those traces (dark trace). Individual pixels are 75 x 75 μm .
- (B)** Left: Summary of the average pA / pixel recorded from pairs of PT and IT cells across individual layers of PFC in response to sCRACM mapping of VM input. Right: Similar for the PT / IT VM input ratio for individual layers. Note the logarithmic axis.
- (C)** Average somatic EPSP evoked at PT and IT cells after apical stimulation of VM axons for experiments shown in Fig. 7 D-F.
- (D)** Average somatic EPSP evoked at PYR cells recorded simultaneously to PT or IT cells after apical stimulation of VM axons for experiments shown in Fig. 7 D-F.
- Values are mean \pm SEM (B left, C, D) or geometric mean \pm 95% CI (B right). * = $p < 0.05$.

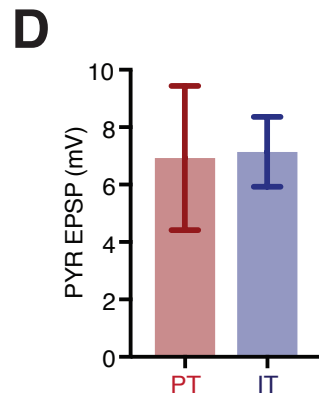
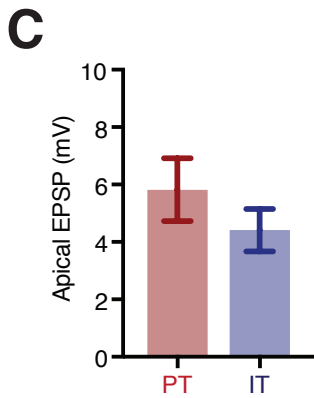
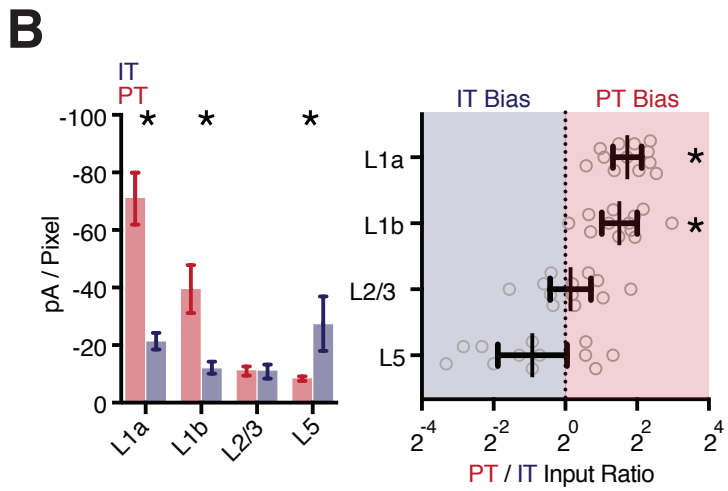
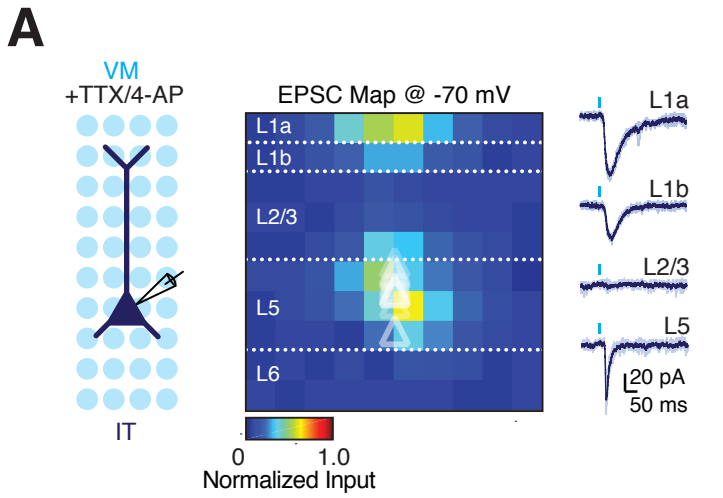
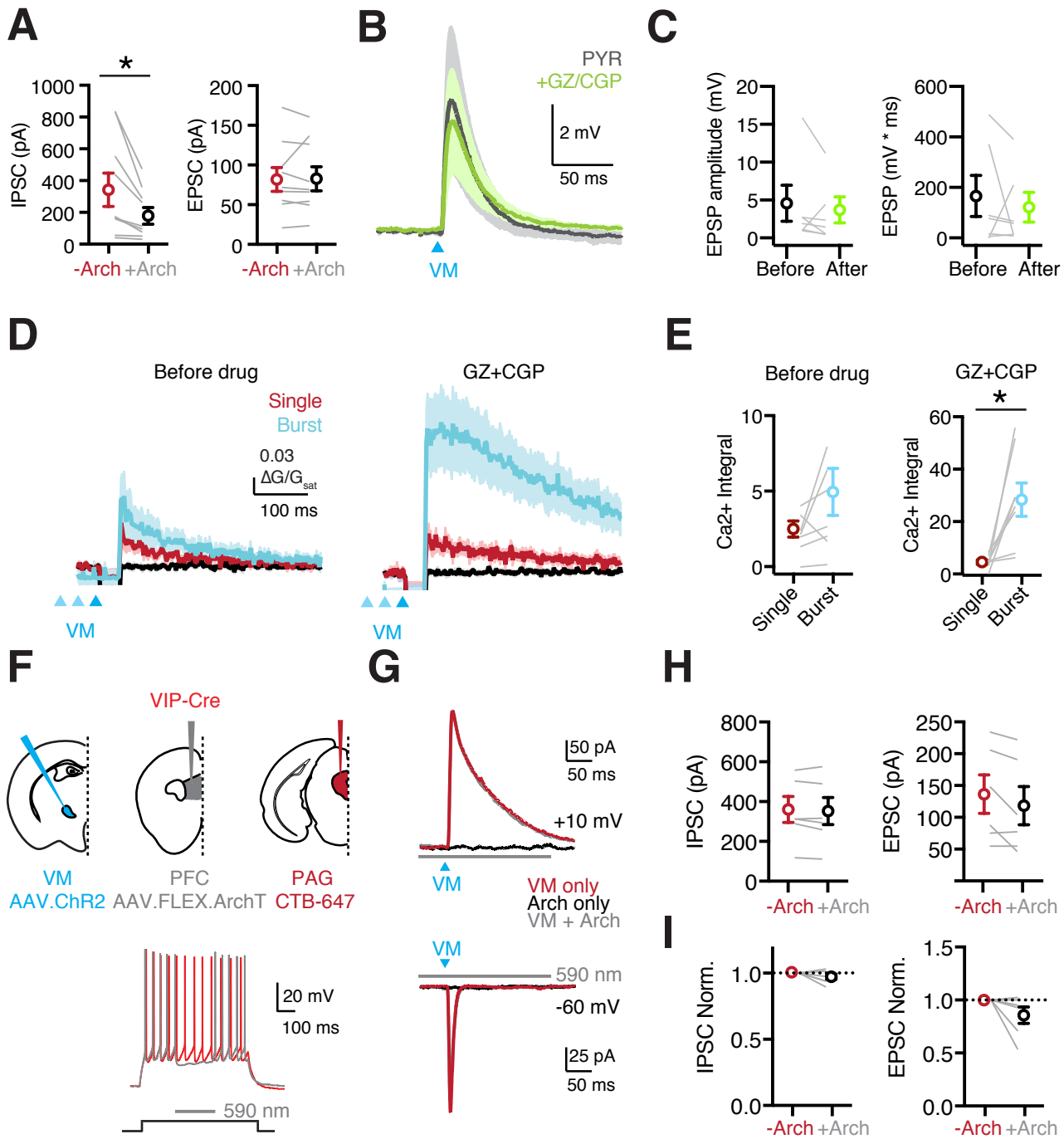


Figure S8. Inhibition shapes responses to VM stimulation, relates to figure 8

- (A) Left: Summary of VM-evoked IPSCs under control conditions and in the presence of ArchT suppression of NDNF+ cells. Right: Similar for VM-evoked EPSCs.
- (B) EPSPs from PYRs recorded at the same time as PT cells in Fig. 8 E-H. Traces are shown before (grey) and after (green) bath application of GABA receptor antagonists GZ and CGP.
- (C) Summary of EPSP amplitude (left) and integral (right) from PYRs before and after bath application of GABA receptor antagonists GZ and CGP.
- (D) Apical dendrite Ca²⁺ signals from PT cells in response to single (red) VM stimulus or a burst (blue) of VM inputs at 50 Hz before (left) and after (right) bath application of GZ and CGP.
- (E) Summary of apical dendrite Ca²⁺ signals from traces in (D) before (left) and after (right) bath application of GZ and CGP.
- (F) Top: Schematic of injections of AAV-ChR2 into VM, AAV-FLEX-ArchT into PFC, and CTB-647 into PAG of VIP-Cre mice. Bottom: VIP+ cell firing evoked by current step in the absence (red trace) and presence (grey trace) of yellow light to activate ArchT (590 nm, 200 ms) and hyperpolarize the VIP+ cell.
- (G) Top: VM-evoked IPSCs measured at +10 mV from PT cells, evoked with blue light to activate ChR2 in the absence (red) or presence (grey) of yellow light to activate ArchT, with black trace showing ArchT-only control. Bottom: Similar but for VM-evoked EPSCs recorded at -60mV.
- (H) Summary of VM-evoked IPSCs (left) and EPSCs (right) without (red) and with (grey) the activation of ArchT showing no effect of ArchT suppression of VIP+ interneurons.
- (I) Summary of normalized VM-evoked IPSC amplitudes (left) and EPSCs (right) from (H).

Values are mean \pm SEM (A, C, E, H, I). * = $p < 0.05$.



Supplemental Table 1	NDNF+		VIP+	
Brain Region	Total Cells Counted	Average % Total	Total Cells Counted	Average % Total
Ipsilateral Cortex				
iACCd	1729	7.43 ± 1.02	2372	10.75 ± 1.06
iACCv	1477	6.47 ± 1.56	1213	4.87 ± 0.86
iAI	472	1.47 ± 1.21	448	1.82 ± 0.25
iAUD	148	0.51 ± 0.28	46	0.19 ± 0.01
iECT/ENT/PERI	104	0.35 ± 0.21	41	0.15 ± 0.05
iGU	9	0.02 ± 0.03	15	0.05 ± 0.03
iIL	1273	4.65 ± 1.89	1252	5.33 ± 0.76
iMOp	497	1.79 ± 0.77	271	1.09 ± 0.13
iMOs	2116	9.06 ± 1.89	974	4.15 ± 0.24
iORB	458	1.58 ± 0.82	1075	4.52 ± 0.38
iPL	3735	25.22 ± 12.27	5601	24.74 ± 2.38
iPTLp	144	0.54 ± 0.35	38	0.15 ± 0.06
iRSP	318	1.19 ± 0.57	157	0.69 ± 0.19
iSSp	407	1.36 ± 0.80	160	0.68 ± 0.23
iSSs	92	0.30 ± 0.19	43	0.17 ± 0.07
iTEA	96	0.27 ± 0.29	16	0.05 ± 0.02
iVlSp	26	0.08 ± 0.06	6	0.02 ± 0.02
Contralateral Cortex				
cACCd	335	1.26 ± 0.46	297	1.16 ± 0.14
cACCv	386	1.57 ± 0.90	203	0.81 ± 0.21
cAI	166	0.51 ± 0.43	87	0.33 ± 0.12
cAUD	3	0.01 ± 0.01	5	0.02 ± 0.01
cECT/ENT/PERI	38	0.13 ± 0.08	15	0.04 ± 0.03
cIL	228	0.77 ± 0.43	147	0.67 ± 0.09
cMOp	12	0.03 ± 0.04	1	0.01 ± 0.01
cMOs	189	0.65 ± 0.36	97	0.41 ± 0.05
cORB	231	0.75 ± 0.47	273	1.15 ± 0.19
cPL	936	4.28 ± 0.26	762	3.03 ± 0.4
cPTLp	3	0.01 ± 0.02	0	0.00
cRSP	11	0.05 ± 0.05	8	0.03 ± 0.02
cSSP	12	0.04 ± 0.03	12	0.06 ± 0.03
cSSs	4	0.01 ± 0.01	2	0.00 ± 0.00
cTEA	3	0.01 ± 0.01	0	0.00
Clastrum				
iCLA	131	0.57 ± 0.18	184	0.64 ± 0.17
cCLA	3	0.01 ± 0.01	2	0.01 ± 0.01
Hippocampus				
iCA1	78	0.61 ± 0.43	372	1.30 ± 0.44
iSUBd	7	0.08 ± 0.06	10	0.03 ± 0.01
iSUBv	34	0.23 ± 0.10	64	0.23 ± 0.13
cCA1	2	0.01 ± 0.01	1	0.00 ± 0.00
Amygdala				
iAAA	7	0.04 ± 0.02	0	0.00
iBLA	65	0.30 ± 0.09	178	0.62 ± 0.21
iBMaa	1	0.00 ± 0.01	3	0.02 ± 0.01
iBMAp	14	0.06 ± 0.02	16	0.05 ± 0.03
iCOA	14	0.04 ± 0.04	17	0.07 ± 0.07
iLA	1	0.00 ± 0.01	1	0.01 ± 0.01
iMEA	5	0.02 ± 0.01	6	0.03 ± 0.02

iPAA	3	0.01 ± 0.02	0	0.00
cBLA	6	0.02 ± 0.02	11	0.03 ± 0.02
cBMAp	2	0.01 ± 0.00	2	0.00 ± 0.00
cCOA	0	0.00	1	0.00 ± 0.00
Olfactory Regions				
DP	72	0.37 ± 0.07	4	0.02 ± 0.01
EP	61	0.22 ± 0.10	46	0.20 ± 0.05
NLOT	8	0.03 ± 0.02	14	0.07 ± 0.02
AON	33	0.20 ± 0.11	32	0.10 ± 0.05
OT	31	0.12 ± 0.04	19	0.09 ± 0.03
iPIR	149	0.58 ± 0.42	14	0.05 ± 0.03
cPIR	4	0.01 ± 0.01	4	0.02 ± 0.01
TR	1	0.00 ± 0.01	0	0.00
TT	195	0.80 ± 0.42	53	0.22 ± 0.10

Supplemental Table 1. Whole-brain inputs from cortical and associated areas, relates to figure 2

Cell counts from whole-brain rabies mapping showing cortical, claustral, hippocampal, amygdalar and olfactory brain regions as specified on the Allen brain atlas (mouse.brain-map.org). Values are shown for NDNF-Cre (n = 3) and VIP-Cre (n = 5) mice. Columns show the total number of rabies labeled cells counted in each brain region summed across all animals and the average % of total input cells associated with each brain region for each genotype.

Values are mean ± SEM.

Supplemental Table 2	NDNF+		VIP+	
Brain Region	Total Cells Counted	Average % Total	Total Cells Counted	Average % Total
Thalamus				
AD	11	0.08 ± 0.04	5	0.02 ± 0.02
AMd	561	3.75 ± 1.62	753	3.26 ± 0.31
AMv	197	1.15 ± 0.34	295	1.08 ± 0.21
AV	0	0.00	20	0.10 ± 0.07
CL	92	0.46 ± 0.05	141	0.55 ± 0.09
CM	74	0.28 ± 0.10	100	0.39 ± 0.06
ETH	0	0.00	17	0.04 ± 0.04
IAD	10	0.13 ± 0.14	2	0.01 ± 0.01
IAM	8	0.03 ± 0.03	3	0.02 ± 0.02
IMD	34	0.12 ± 0.06	61	0.25 ± 0.11
LD	9	0.03 ± 0.02	1	0.00 ± 0.00
LP	81	0.37 ± 0.02	32	0.14 ± 0.03
MD	705	3.30 ± 0.03	2126	8.96 ± 0.60
PT	73	0.37 ± 0.02	112	0.41 ± 0.09
PCN	1	0.00 ± 0.01	5	0.02 ± 0.02
PF	178	0.80 ± 0.32	239	0.94 ± 0.15
PO	66	0.22 ± 0.14	41	0.19 ± 0.02
PR	2	0.01 ± 0.01	14	0.05 ± 0.02
PVT	20	0.15 ± 0.10	43	0.19 ± 0.09
RE	143	0.55 ± 0.24	78	0.33 ± 0.09
RH	49	0.23 ± 0.00	52	0.22 ± 0.04
SMT	46	0.19 ± 0.06	80	0.33 ± 0.09
SPA	5	0.01 ± 0.02	6	0.01 ± 0.01
SPFM	15	0.04 ± 0.05	4	0.01 ± 0.01
VAL	386	1.75 ± 0.22	654	3.09 ± 0.41
VM	1072	4.51 ± 0.97	817	3.63 ± 0.64
VPL	67	0.27 ± 0.10	100	0.48 ± 0.14
VPM	36	0.22 ± 0.09	35	0.19 ± 0.10
Hypothalamus				
ARH	1	0.00 ± 0.00	9	0.04 ± 0.01
AVP	4	0.01 ± 0.01	0	0.00
DMH	0	0.00	3	0.02 ± 0.01
LHA	41	0.30 ± 0.19	73	0.31 ± 0.08
LM	0	0.00	1	0.01 ± 0.01
LPO	17	0.09 ± 0.02	13	0.07 ± 0.04
MM	3	0.01 ± 0.02	0	0.00
MPO	3	0.01 ± 0.01	17	0.07 ± 0.07
PH	23	0.08 ± 0.05	17	0.09 ± 0.03
PVH	1	0.00 ± 0.00	3	0.01 ± 0.01
PVp	2	0.01 ± 0.00	1	0.00 ± 0.00
RCH	1	0.00 ± 0.01	6	0.01 ± 0.01
STN	1	0.00 ± 0.01	1	0.01 ± 0.01
SUM	6	0.02 ± 0.02	8	0.03 ± 0.03
TU	0	0.00	3	0.01 ± 0.01
VMH	0	0.00	1	0.01 ± 0.01
ZI	12	0.06 ± 0.01	7	0.03 ± 0.01
Striatum & Pallidum				
BST	1	0.00 ± 0.00	4	0.02 ± 0.02
DMSTR	2	0.01 ± 0.00	3	0.01 ± 0.01

GP	92	0.52 ± 0.15	200	0.85 ± 0.13
LS	110	0.44 ± 0.25	29	0.11 ± 0.06
MS	69	0.28 ± 0.12	45	0.21 ± 0.06
NAC	7	0.026 ± 0.02	8	0.04 ± 0.02
NDB	316	1.61 ± 0.34	233	1.0 ± 0.16
SF	2	0.01 ± 0.01	0	0.00
SH	31	0.12 ± 0.09	2	0.01 ± 0.00
SI	81	0.40 ± 0.04	144	0.60 ± 0.04
Mid & Hindbrain				
EW	1	0.00 ± 0.00	0	0.00
IPN	2	0.01 ± 0.01	3	0.02 ± 0.01
LC	3	0.01 ± 0.02	3	0.01 ± 0.01
LDT	0	0.00	3	0.02 ± 0.02
MRN	2	0.01 ± 0.01	1	0.01 ± 0.01
PAG	4	0.01 ± 0.01	3	0.01 ± 0.01
MEPO	1	0.02 ± 0.02	0	0.00
PB	6	0.02 ± 0.02	1	0.00 ± 0.00
PPN	3	0.03 ± 0.02	5	0.02 ± 0.01
Raphe	29	0.14 ± 0.03	47	0.18 ± 0.05
RM	1	0.00 ± 0.01	0	0.00
RN	0	0.00	1	0.00 ± 0.00
SNc	0	0.00	5	0.02 ± 0.01
SNr	3	0.01 ± 0.01	1	0.00 ± 0.00
TRN	0	0.00	1	0.01 ± 0.01
VTA	42	0.17 ± 0.03	55	0.23 ± 0.06
VTN	0	0.00	1	0.01 ± 0.01

Supplemental Table 2. Whole-brain inputs from thalamic and subcortical areas, relates to figure 2

Cell counts from whole-brain rabies mapping showing thalamic, hypothalamic, striatal & pallidal and midbrain & hindbrain regions as specified on the Allen brain atlas (mouse.brain-map.org). Values are shown for NDNF-Cre (n = 3) and VIP-Cre (n = 5) mice. Columns show the total number of rabies labeled cells counted in each brain region summed across all animals and the average % of total input cells associated with each brain region for each genotype.

Values are mean ± SEM.